Analysis of the Surfaces of Wood Tissues and Pulp Fibers Using Carbohydrate-Binding Modules Specific for Crystalline Cellulose and Mannan

Lada Filonova,*,† Åsa M. Kallas,‡ Lionel Greffe,‡ Gunnar Johansson,§ Tuula T. Teeri,‡ and Geoffrey Daniel†

Department of Wood Science, Swedish University of Agricultural Sciences, Uppsala, Sweden, Department of Biotechnology, Royal Institute of Technology, AlbaNova University Centre, Stockholm, Sweden, and Department of Biochemistry, Uppsala University, Sweden

Received June 30, 2006; Revised Manuscript Received October 6, 2006

Carbohydrate binding modules (CBMs) are noncatalytic substrate binding domains of many enzymes involved in carbohydrate metabolism. Here we used fluorescent labeled recombinant CBMs specific for crystalline cellulose ($CBM1_{HjCel7A}$) and mannans ($CBM27_{TmMan5}$ and $CBM35_{CjMan5C}$) to analyze the complex surfaces of wood tissues and pulp fibers. The crystalline cellulose $CBM1_{HjCel7A}$ was found as a reliable marker of both bacterially produced and plant G-layer cellulose, and labeling of spruce pulp fibers with $CBM1_{HjCel7A}$ revealed a signal that increased with degree of fiber damage. The mannan-specific $CBM27_{TmMan5}$ and $CBM35_{CjMan5C}$ CBMs were found to be more specific reagents than a monoclonal antibody specific for (1→4)-*β*-mannan/galacto-(1→4)-*β*-mannan for mapping carbohydrates on native substrates. We have developed a quantitative fluorometric method for analysis of crystalline cellulose accumulation on fiber surfaces and shown a quantitative difference in crystalline cellulose binding sites in differently processed pulp fibers. Our results indicated that CBMs provide useful, novel tools for monitoring changes in carbohydrate content of nonuniform substrate surfaces, for example, during wood or pulping processes and possibly fiber biosynthesis.

Introduction

Understanding the biosynthesis, composition, ultrastructure, properties, and microbial decay of plant cell walls is one of the major challenges for future engineering of quality parameters of industrial crop plants for improved utility of the raw material.[1−3] At the fundamental research level, specific markers for carbohydrates are needed to improve the interpretation of data obtained by reverse genetic studies of cell wall synthesis and modification.[4,5] In practical applications, the determination of the carbohydrate composition on pulp fiber surfaces can help to understand the relationships between fiber processing conditions versus fiber performance.[6,7] Spatial analyses combined with high-resolution imaging, often aided by the use of specific antibodies, have been the methods of choice to identify different domains of carbohydrates and proteins within cell walls.[8−11] Immunolocalization studies by light, confocal, and electron microscopy require well-characterized and highly specific polyclonal or monoclonal antibodies. While antibodies are generally easy to generate against protein antigens, most carbohydrates must be conjugated to antigenic carrier proteins for efficient immunization.[12] In the case of complex carbohydrate polymers in plant cell walls, purification of either the native antigen or a recombinant copy in sufficient amount is often a limiting step of immunization. This is since some of the carbohydrates occur in the cell walls in low concentrations and may suffer chemical changes due to chemical extraction required for their purification. Furthermore, when intact antibodies are used together with secondary conjugates, problems often arise in resolution owing to the large size of the antibody complex leading to sterical hindrance of the probes.

In nature, lectins and other carbohydrate binding proteins are commonly used for carbohydrate recognition.[13,14] Enzymes degrading plant cell wall polysaccharides are rich sources of highly specific noncatalytic carbohydrate binding modules (CBMs).[15−19] Based on amino acid sequence and structural similarities, CBMs have been divided into 45 families (http://afmb.cnrs-mrs.fr/CAZY/) and classified into three main groups. Type A CBMs exhibit affinity toward insoluble crystalline cellulose and/or chitin and have planar, hydrophobic binding surfaces.[15,20−23] Type B CBMs have cleft-shaped substrate binding-sites decorated with aromatic amino acids and typically bind soluble polysaccharides. Type C CBMs resemble lectins and bind shorter substrates such as mono-, di-, and trisaccharides. Many CBMs have been experimentally found to target components of plant cell walls such as crystalline and amorphous cellulose and different types of mannans and xylans.[15,19]

Biotechnological applications of CBMs so far culminate on their ability to serve as tags for the purification and immobilization of fusion proteins.[24] However, the CBM derived from the cellulase Cel7D of *Phanerochaete chrysosporium* ($CBM1_{PcCel7D}$) has been previously covalently labeled with fluorescein isothiocyanate (FITC) and used to detect cellulose in never-dried spruce and birch wood sections as well as pulp fibers.[25] Similarly, the specificity of recombinant CBMs from glycoside hydrolases in families GH2A, GH6, and GH29 have been investigated in order to develop specific probes to study developmental and functional aspects of plant cell walls.[19] Recently it has been shown that

* To whom correspondence should be addressed. E-mail: lada.filonova@trv.slu.se.
† Swedish University of Agricultural Sciences.
‡ AlbaNova University Centre.
§ Uppsala University.

10.1021/bm060632z CCC: $37.00
Published on Web 12/13/2006

Table 1. Chemical Composition for the Different Nonuniform Substrates

chemical composition (%)	pulp PS[a]	pulp PH[b]	BMCC	*Populus tremuloides* normal wood	*Populus tremuloides* tension wood	Betula verrucosa	Pinus sylvestris
cellulose	76.0	86.8	100	42.7	54.0	53.7	61.8
hemicelluloses	19.9	8.7	–	10.7		25.7	24
glucoman./mannan	12.7	4.6	–	5.2	2.0	3.6	24.0
xylan	7.2	4.1	–	29.2	23.8	40.9	7.9[c]
lignin	4.1	4.6	–	20.9	16.8	15.7	26.1
reference	10	10	34	35, 36	35, 36	37, 38	37, 39, 40

[a] Polysulfide pulping method. [b] Prehydrolyzed pulping method. [c] Xylan in cellulose as % cellulose.

six different xylan binding modules from CBM families 2b, 4, 6, 15, 22, and 35 exhibit a range of specificities for natural ligands in plant cell walls.[26] The data obtained in this landmark contribution provides the first concrete demonstration that CBMs represent new versatile tools for probing the carbohydrate content of cell walls.

Here we have used labeled CBM1$_{Hj\text{Cel7A}}$ from the Cel7A of *Hypocrea jecorina* (formerly *Trichoderma reesei*,[27,28] CBM27$_{Tm\text{Man5}}$ from *Thermotoga maritima* Man5[29] and CBM35$_{Cj\text{Man5C}}$ from *Cellvibrio japonicus* Man5C[30] to map the carbohydrate distribution of crystalline cellulose and mannans on wood cell walls and pulp fibers. The data hereby obtained shows that cellulose-binding modules can be used to detect areas of crystalline cellulose with high precision. Furthermore, comparative analysis shows superior performance of the mannan-binding modules relative to mannan specific antibodies.

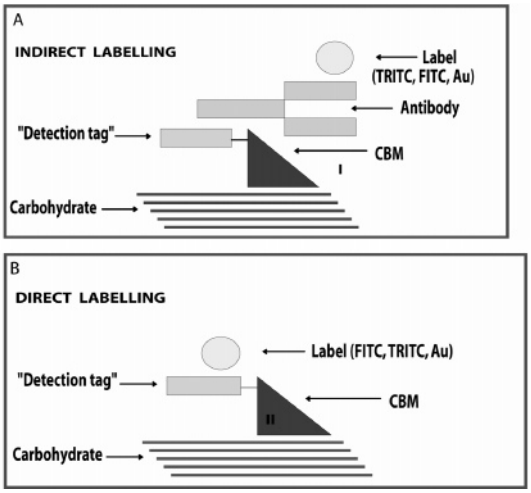

Figure 1. The two principles employed for carbohydrate mapping using CBM-fusion proteins.

Experimental Section

Production, Characterization, and Labeling of the Recombinant CBMs. The CBM1 from *H. jecorina* Cel7A (ZZ-CBM1$_{Hj\text{Cel7A}}$) fused to the ZZ domain of the *Staphylococcus aureus* protein A and CBM27 from *T. maritima* Man5 (CBM27$_{Tm\text{Man5}}$) and CBM35 from *C. japonicus* Man5C (CBM35$_{Cj\text{Man5C}}$) both fused to polyhistidine tags were expressed and purified as described earlier.[28,29,31] The binding properties of the ZZ-CBM1$_{Hj\text{Cel7A}}$ on bacterial microcrystalline cellulose (BMCC) and Avicel were determined according to Srisodsuk et al.[32] Binding of His$_6$-CBM27$_{Tm\text{Man5}}$ and CBM35$_{Cj\text{Man5C}}$-His$_6$ modules to glucomannan was confirmed by affinity gels as previously described.[33]

In order to label the CBM with fluorescein isothiocyanate (FITC), 1 mL of a FITC stock solution (20 mM in 10 mM $NaHCO_3$) was mixed with 8.5 mL of protein solution (60 μg/mL of ZZ-CBM1$_{Hj\text{Cel7A}}$ in 10 mM $NaHCO_3$) and 0.5 mL of buffer (10 mM $NaHCO_3$) followed by stirring for 3 h at room temperature. The nonbound FITC molecules were removed by washing twice with 10 mL of 200 mM ammonium acetate (pH 5), followed by concentration to 500 μL. The washing and concentration steps were carried out using Centricon Plus-20 filtering devices (Millipore). Incorporation of FITC molecules was confirmed by MS analysis and resulted in 1−4 FITC molecules per CBM molecule.

Substrates. We have used a range of substrates representing different content and combinations of pure crystalline cellulose, hemicellulose, and lignin based on previous data on substrate chemical composition (Table 1).

"Never-dried" bacterial microcrystalline cellulose (BMCC) was obtained by cultivating *Acetobacter xylinum* (ATCC R N1024) in liquid peptone/yeast extract/mannitol medium.[41] Cellulose pellicles produced on the surface of the medium (7-day-old) were harvested, and the cellulose was purified using modified non-organic alkaline-acidic treatment.[34] Serial wood sections (15 μm) from poplar (*Populus tremuloides*), birch (*Betula verrucosa Ehrh.*), and pine (*Pinus sylvestris* L.) were prepared using a Leitz microtome. For poplar samples, mild delignification was performed using a 1:1 (v/v) mixture of H_2O_2 and concentrated acetic acid.[42] Oxygen bleached and unbleached spruce (*Picea abies* Karst.) kraft pulp with high hemicellulose content (polysulfide pulping method, PS) and low hemicellulose content (prehydrolysed pulping method, PH) were obtained as described previously.[43]

A constant dry weight of different pulp fibers was used for all experimental series, and alternate sections from the same wood specimens were used for every CBM and antibody labeling experiment.

Sample Labeling with CBMs. All labeling experiments were carried out in triplicate using Eppendorf tubes. Nonspecific binding of the CBMs was prevented by the initial blocking of all samples with 5% (w/v) ovalbumin in 50 mM sodium acetate buffer (pH 5.5). In all cases, a range of CBM concentrations (1, 5, 10, 20, 30, 50 μM) were tested for each CBM in order to find the lowest feasible working concentration and to reduce background fluorescence.

Detection of CBM binding was achieved using two approaches of carbohydrate mapping, which are termed "indirect" and "direct" labeling. Indirect labeling is based on antibody-mediated labeling of the CBMs bound to the substrate (Figure 1A). Direct labeling involved substrate labeling with CBM directly conjugated with a marker molecule (Figure 1B).

Two different methods were adopted for indirect labeling: (i) sequential treatment of the samples with the CBMs, followed by detection of the bound CBM by an IgG-FITC/tetramethyl rhodamine isothiocyanate (TRITC) conjugate; and (ii) treatment of the samples with a previously complexed CBM-IgG-FITC/TRITC conjugate.[24]

With the "indirect" CBM binding approach (i), 10 μM ZZ-CBM1$_{Hj\text{Cel7A}}$, 15 μM His$_6$-CBM27$_{Tm\text{Man5}}$, or 4 μM CBM35$_{Cj\text{Man5C}}$-His$_6$ in 50 mM sodium acetate buffer (pH 5.5) containing 1% (w/v) ovalbumin (Sigma) were incubated with the target substrates for for 4−5 h at room temperature (RT). Samples were then washed twice

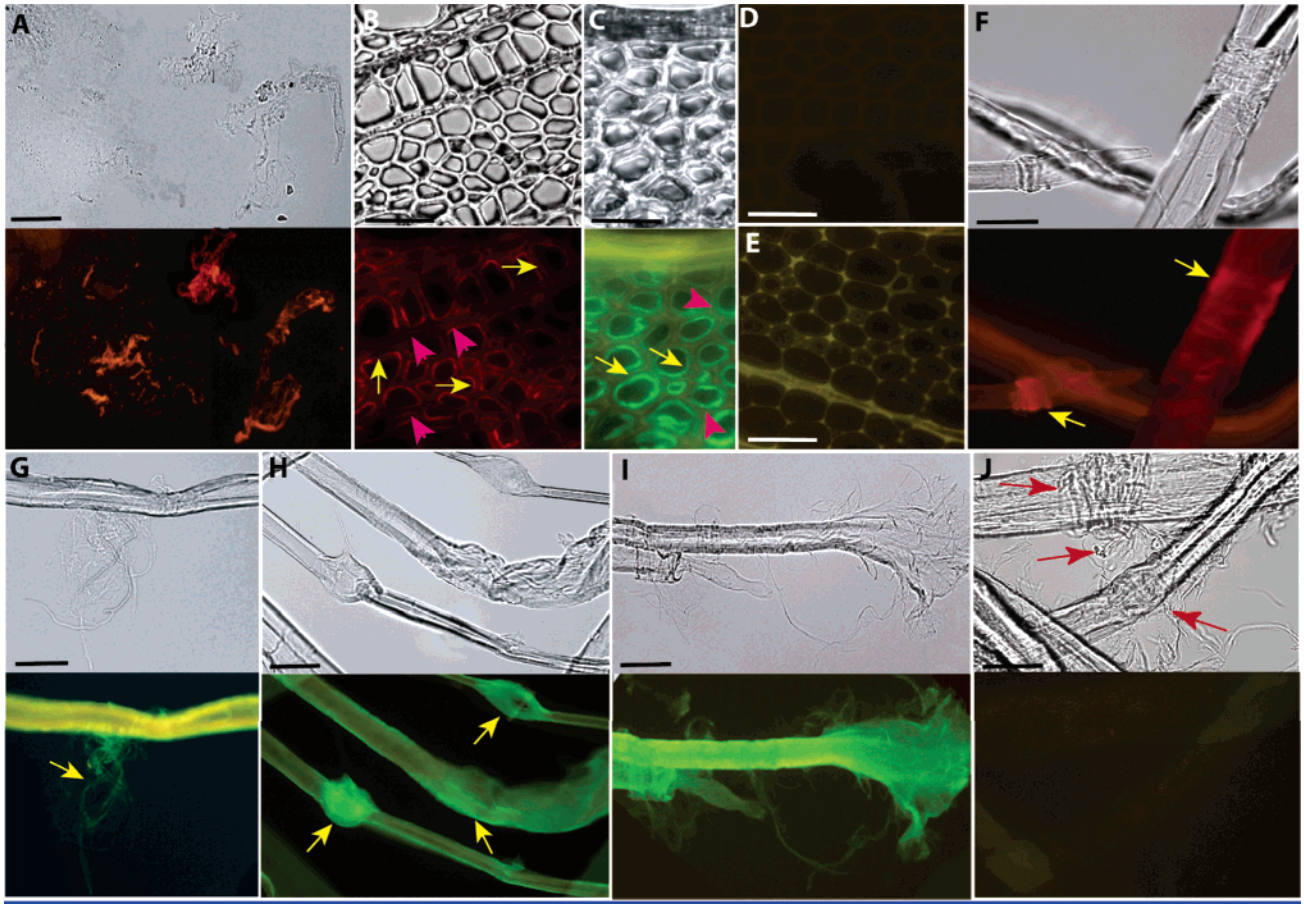

Figure 2. Binding of CBM1$_{HjCel7A}$ to purified microcrystalline cellulose from *Acetobacter xylinus* (BMCC) and to different wood and pulp fiber samples. (A) Binding of TRITC-CBM1$_{HjCel7A}$ to the cellulose microfibrils of BMCC. (B, C) Poplar and birch tension wood fibers (yellow arrows—labeling of G-layer, pink arrowheads—labeling of S1 cell wall layer). (D) Poplar negative control, staining with TRITC-conjugated IgG. (E) Birch negative control, staining by FITC-conjugated IgG. (F) The S1-layer of spruce PH pulp fiber surfaces particularly at sites of dislocations shows strong labeling (arrows). (G−I) Labeling intensity on spruce PS pulp fibers increased with level of fiber damage (i.e., sites of swelling, dislocations, kinks), surface fibrillation, and fiber rupture. (J) Fibers negative control, spruce PS pulp fibers stained by FITC-conjugated Protein A (red arrows show remaining S1-layer on the fiber surface, swelling, fiber surface fibrillation). The corresponding light microscope bright field images of the same section or fiber areas of the samples are shown in A−C, F−J above the fluorescent images. Scale bars = 100 μm for A, G−I; 50 μm for B−F, J.

with active stirring in 50 mM sodium acetate buffer (pH 5.5) for 20 min each. Thereafter, samples treated with the ZZ-CBM1$_{HjCel7A}$ were incubated for 1 h at RT with FITC or TRITC-conjugated rabbit anti-mouse antibody (Sigma, recognizing ZZ-domain) diluted 1:500 with 20 mM phosphate buffer (pH 7.2). Samples treated with His$_6$-CBM27$_{TmMan5}$ and CBM35$_{CjMan5C}$-His$_6$ were incubated for 1 h in RT with mouse monoclonal anti-Penta-His antibodies available as Alexa Fluor 488 (excitation max. 494 nm) and Alexa Fluor 555 (excitation max. 555 nm) conjugates (Quagen). The antibody conjugates were used in a 1:500 dilution in PBS (pH 7.2).

With the "indirect" approach (ii),[28] equal volumes of the CBMs (in final concentrations given above) and 12 μg/mL FITC-conjugated anti-mouse IgG (Sigma) or Penta-His Alexa Fluor 488/Penta-His Alexa Fluor 555 conjugates in 50 mM sodium acetate buffer (pH 5.5) containing 1% (w/v) ovalbumin were mixed and preincubated for 1 h at RT. Samples were then treated with the CBM-antibody mixtures for 2 h at RT followed by three washes with water (20 min each step). Samples labeled with only the FITC-conjugated rabbit anti-mouse IgG, Penta-His Alexa Fluor 488, or Penta-His Alexa Fluor 555 (all diluted 1:500 in PBS) were used as negative controls.

In the case of "direct" labeling using CBMs conjugated with FITC, samples were treated by 0.5 μM ZZ-CBM1$_{HjCel7A}$ labeled with FITC (see M & M, recombinant CBMs) in 50 mM sodium acetate buffer (pH 5.5) supplemented with 1% (w/v) ovalbumin for 4 h at RT or overnight at 4 °C. FITC-conjugated Protein A (0.5 μM, Sigma) in 50 mM sodium acetate buffer (pH 5.5) containing 1% (w/v) ovalbumin was used as negative control.

Sample Labeling with (1→4)-β-Mannan/Galacto-(1→4)-β-mannan Antibodies. Samples were blocked in PBS containing 5% (w/v) bovine serum albumin (BSA, Sigma) for 30 min, and thereafter they were rinsed three times with PBS (10 min each) at RT and incubated overnight at 4 °C with mouse monoclonal antibody (1→4)-β-mannan/galacto-(1→4)-β-mannan antibody (Biosupplies Australia Pty Ltd.) diluted 1:250 in PBS with 1% (w/v) BSA (Sigma, pH 7.2). All subsequent procedures were performed at RT. After two washes in PBS (30 min each), samples were labeled using FITC-conjugated anti-mouse IgG diluted 1:500 in PBS for 1 h and finally washed three times in distilled water (10 min each step). All labeling was done in triplicate.

Fluorescent Microscopy. All samples were placed on object glasses mounted in Fluorsave (Calbiochem, CA), covered by coverslips and examined by fluorescent microscopy (Leica, Germany) using a standard set of filters for FITC, TRITC (rhodamine), or Alexa Fluor 488, 555. Images were recorded via a CCD camera (Leica DC 300F, Microsystem) using a digital imaging system for professional microscopy (Leica Microsystem Ltd., 2001) with one exposure time (3.5 s) for all samples in order to detect differences in signal intensity.

Determination of Adsorption Isotherm Parameters on Avicel as a Standard Substrate. ZZ-CBM1$_{HjCel7A}$ in concentrations ranging from ca. 1−20 μM were incubated in Eppendorf tubes with 1.5 mg Avicel

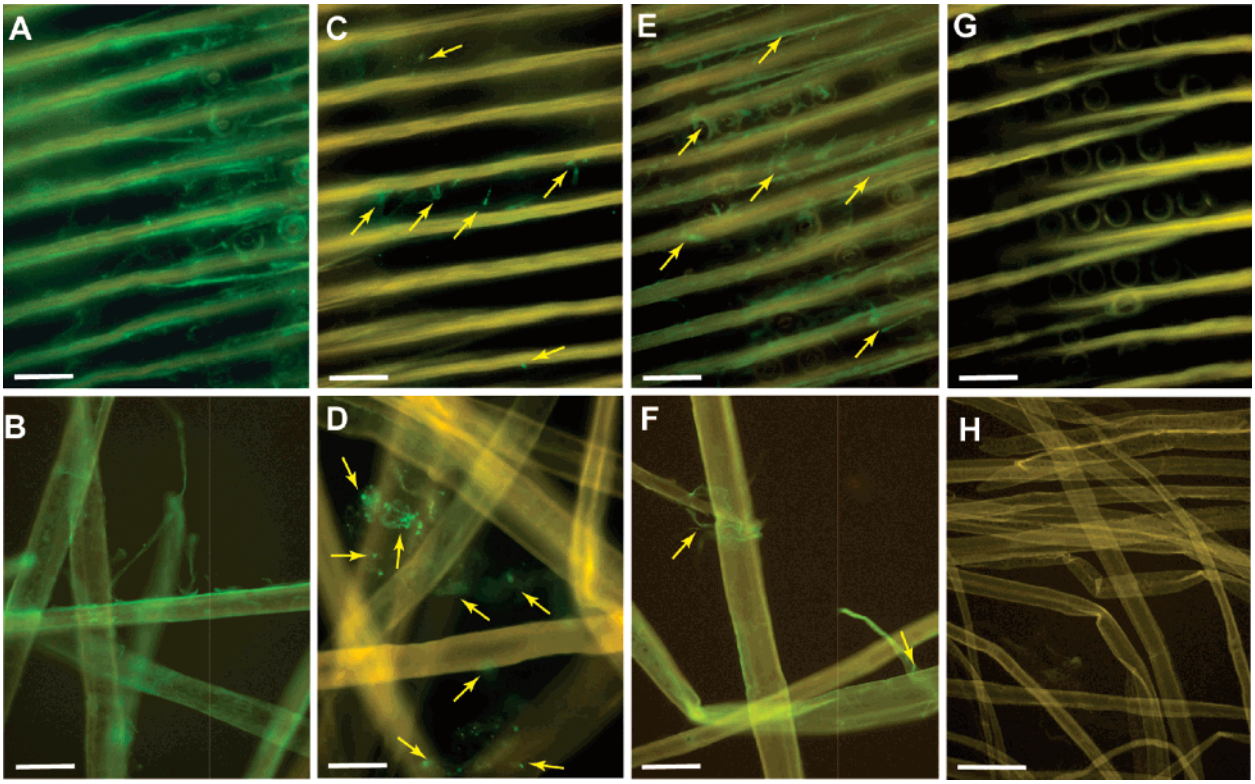

Figure 3. Comparison of labeling of a (1→4)-β-mannan/galacto-(1→4)-β-mannan antibody and mannan-specific CBMs using spruce wood sections and spruce pulp fibers. (A, B) CBM35$_{CjMan5C}$-His6 labeling showed intense labeling of both spruce sections and spruce pulp fiber surfaces. (C, D) His6-CBM27$_{TmMan5}$ showed restricted labeling to highly fibrillated parts on spruce pulp fibers and that exposed during sectioning wood samples. (E, F) Uniform but weak labeling of spruce sections and pulp fibers using a monoclonal antibody to (1→4)-β-mannan/galacto-(1→4)-β-mannan. (G, H) negative controls (G, labeling with FITC-conjugated anti-mouse IgG; H, labeling with Penta-His Alexa Fluor 488). Scale bars = 100 μm for A−F, 200 μm for H.

(5 mg/mL) in 300 μL of 50 mM PBS pH 7.1 at RT overnight. Samples were then centrifuged for 10 min at 13 000 rpm in a Biofuge pico (Heraeus Instruments). The absorbance of the supernatants at 492 nm was measured in a Shimadzu UV-2501PC spectrophotometer and used for calculation of supernatant concentration using the extinction coefficient $\epsilon_{492,1cm} = 79\ 000\ M^{-1}\ cm^{-1}$. The amount of protein bound was calculated from the difference between the initial protein concentration and that observed in the supernatant allowing for the construction of an adsorption isotherm (Figure 4). K_d and B_{max} were calculated from the standard expression by nonlinear least-square regression using the program Axum 6.0 (MathSoft inc.):

$$\text{Bound} = B_{max}\frac{\text{Free}}{\text{Free} + K_d}$$

where B is amount of bound CBM1$_{HjCel7A}$ (mol/g) and Free is the concentration of unbound CBM1$_{HjCel7A}$ in the supernatant (M).

Fluorescence Based Quantitative Analysis of Pulp Samples. Bleached and unbleached PS pulps (5 mg dry weight) were incubated with 1 mL of 253 nm ZZ-CBM1$_{HjCel7A}$ solutions (A_{492}= 0.020) overnight at RT and fluorescence was measured in an Aminco SPF-500 spectrophotofluorimeter employing the Ratio mode using mirrored cuvets with 1 cm path length. Excitation and emission wavelengths were set at 492 and 520 nm, respectively, with slit widths set at 2 nm. The fluorescence F was used to calculate the concentration in the supernatant after incubation according to

$$[\text{CBM}]_{sup} = F_{sup}\frac{[\text{CBM}]_{ini}}{F_{ini}}$$

where $[\text{CBM}]_{ini}$ and $[\text{CBM}]_{sup}$ are concentrations of CBM1$_{HjCel7A}$ before and after sample incubation, respectively (nM); F_{ini} is the initial fluorescence, and F_{sup} is the fluorescence after sample incubation. Quintuples of samples were employed.

Results and Discussion

Detection of Crystalline Cellulose on Tension Wood Tissues and Pulp Fiber Surfaces. CBM1$_{HjCel7A}$ has been assigned to the type A binding modules that bind specifically to insoluble (crystalline) cellulose or chitin[28,44,45] with no detectable disruption of the cellulose structure.[44−47] Biochemical binding studies are normally carried out using pure carbohydrates as model substrates. However, plant cell walls contain a combination of cellulose, lignin, hemicelluloses, and other cell wall components particularly wood and thus do not provide uniform substrates. Therefore experimental samples serving as positive controls for CBM1$_{HjCel7A}$ were also required.

Pure bacterial microcrystalline cellulose obtained from *Acetobacter xylinum* cultures[34] and the G-layers from poplar and birch tension wood fibers contain almost exclusively pure cellulose with very high crystallinity.[48] As shown in Figure 2A−C, treatment of BMCC and tension wood fibers with the labeled ZZ-CBM1$_{HjCel7A}$ resulted in strong specific labeling. In particular, the G-layer lining the inner lumen wall in poplar and birch fibers showed a strong green or red fluorescence in transverse sections (Figure 2B,C, arrows). In addition, weaker labeling was also shown for the outer secondary S1 layer (Figure 2B,C) that lies between the inner secondary (S2 + G-layer) wall and the compound middle lamella region (Figure 2B,C; arrowheads). Accessibility to substrate binding sites is an important factor that affects the intensity of CBM labeling in native carbohydrate structures. With cellulose, accessibility is

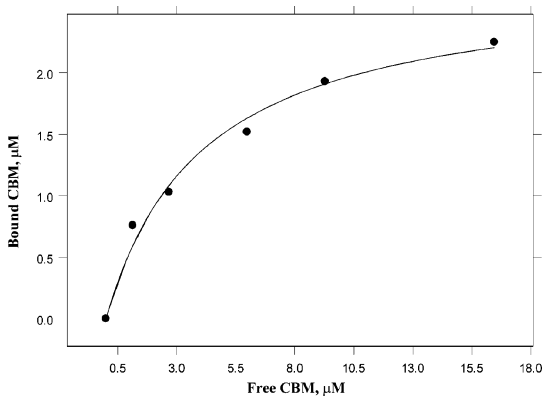

Figure 4. Binding isotherm for ZZ-CBM1$_{Hj\text{Cel7A}}$ from *H. jecorina* on Avicel.

governed either by cellulose orientation (microfibril angle, MFA) or obstruction by other cell wall components (like hemicelluloses and lignin). The MFA (microfibril angle) of cellulose in the G-layer is known to lie almost parallel with the fiber axis, while the S1 layer has almost a perpendicular orientation.[49] Since both G-layer and S1 layers were labeled—although the G-layer was much more intense—the MFA may not be critical for labeling by CBM1$_{Hj\text{Cel7A}}$. The result suggests that the binding of CBM1$_{Hj\text{Cel7A}}$ is mainly governed by the high concentration of crystalline cellulose in the S1 layer (ca. 60%[37]) and G-layer.[50] Interestingly, no labeling by the ZZ-CBM1$_{\text{HjCel7}}$ was detected in tension wood G-layer samples after mild delignification using (1:1) H_2O_2−HoAc (data not shown). As suggested earlier, delignification may change the crystallinity of cellulose[51] thereby modifying the structural organization of the ZZ-CBM1$_{\text{HjCel7}}$ binding site.

The frequency and intensity of labeling of spruce kraft pulp fibers by CBM1$_{Hj\text{Cel7A}}$ appeared correlated with the availability of exposed crystalline cellulose on the fiber surfaces. More intensive labeling was concentrated to S1-layer remaining on the fiber surfaces (Figure 2F) and damaged fiber areas (Figure 2G−J). As described previously for CBM1$_{Pc\text{Cel7D}}$[25], the increased labeling with CBM1$_{Hj\text{Cel7A}}$ was also detected at swollen or ruptured fiber areas (Figure 2H), sites of dislocations, kinks (Figure 2G,H), and external fiber fibrillation (Figure 2I). Even though the interaction of CBM1$_{Hj\text{Cel7A}}$ with cellulose has been shown to be fully reversible, and the CBM can be eluted from cellulose by simple washing,[44] the labeling of the wood tissues and the pulp fibers was found stable for at least 72 h. Fluorescence signals/background was not detected in control samples stained with TRITC-conjugated anti-mouse IgG (Figure 2D) or FITC-conjugated Protein A (Figure 2E,J).

Comparative Labeling of Wood Tissues and Pulp Fibers by Mannan Specific Antibodies and Mannan-Binding Modules. Different mannan-binding modules are known to exhibit different binding specificity and capacity.[29,30,52−55] With our work, CBM35$_{Cj\text{Man5C}}$ showed relatively uniform binding on the spruce semi-thin sections and pulp fiber substrates used (Figure 3A,B), whereas CBM27$_{Tm\text{Man5}}$ bound only to the highly fibrillated parts of fibers and sections (Figure 3C,D; arrows). Similar results were obtained using both protocols of labeling with two different fluorophores (TRITC and FITC).

The binding specificity of CBMs depends on complementary interaction between the structure and conformation of the substrate and the architecture of the actual CBM binding site. Both CBM27$_{Tm\text{Man5}}$ and CBM35$_{Cj\text{Man5C}}$ belong to the large CBM superfamily with a β-jelly-roll fold.[15] CBM35$_{Cj\text{Man5C}}$ from *C. japonicus* has been proven to bind specifically to mannan and glucomannan.[31,30,56] In contrast CBM27$_{Tm\text{Man5}}$ from *T. maritime* has shown to be specific to the manno-oligosaccharides, carob-galactomannan, and konjac glucomannan.[30] Thus the variations in labeling observed with the present samples is most likely related to the availability of the substrate preferences.

Table 2. B_{max} (pmol mg^{-1}) for PS and PS Bleached Spruce Pulp[a]

sample	F_{ini}	F_{sub}	A_{ini}	$[CBM]_{ini}$, nM	$[CBM]_{sub}$, nM	B_{max}, pmol mg^{-1}
ZZ-CBM1$_{Hj\text{Cel7A}}$	40.3		0.02	253		
PS		31.1			195	240 ± 48
PS bleached		36.3			228	100 ± 20

[a] F_{ini}, initial fluorescence of ZZ-CBM1$_{Hj\text{Cel7A}}$ solution; F_{sub}, fluorescence after incubation of substrate in ZZ-CBM1$_{Hj\text{Cel7A}}$ solution; A_{ini}, initial absorbance of ZZ-CBM1$_{Hj\text{Cel7A}}$ solution; $[CBM]_{ini}$, initial concentration of ZZ-CBM1$_{Hj\text{Cel7A}}$; $[CBM]_{sub}$, final concentration of ZZ-CBM1$_{Hj\text{Cel7A}}$ in supernatant after incubation with substrate.

In addition, the three-dimensional structures of the two mannan-binding modules used in this study[29,56] reveal two different binding sites, which also can explain the differences in binding. With CBM27$_{Tm\text{Man5}}$, the substrate-binding site is located on the concave surface of the protein while the binding site of CBM35$_{Cj\text{Man5C}}$ is formed by loops connecting two β-sheets. Furthermore, the binding site of CBM35$_{Cj\text{Man5C}}$ undergoes significant conformational changes upon substrate binding. This flexibility may explain why CBM35$_{Cj\text{Man5C}}$ appears to bind more strongly to substituted substrates than CBM27$_{Tm\text{Man5}}$.[56] In the case of CBM27$_{Tm\text{Man5}}$, the binding interaction seems to be dominated by hydrophobic stacking between one aromatic amino acid on the CBM and one mannose unit on the substrate. Thus it is reasonable to assume that an increased degree of substitution on the substrate may interfere with such an interaction.

The efficiency of mannan labeling by the CBM35$_{\text{CjMan5C}}$ was more apparent than (1→4)-β-mannan/galacto-(1→4)-β-mannan antibody labeling of the same samples (Figure 3E,F), while labeling by CBM27$_{Tm\text{Man5}}$ was comparable to antibody labeling both for spruce wood sections and pulp fiber samples. No fluorescence signals/background was detected in control samples stained only with FITC-conjugated anti-mouse IgG (Figure 3G,H).

Analysis of Exposed Available Substrate on Pulp Fiber Surfaces. A fluorometric adsorption assay based on measuring the fluorescence of unbound protein remaining in the supernatant of eppendorf tubes during labeling was used for semiquantitative binding analysis of CBMs bound to pure substrates.[20,25,27]

The bulk chemical analysis of the carbohydrate content of complex substrates such as kraft pulp or wood samples provides no information of its surface carbohydrate architecture. Thus the possibility to quantify the availability of different carbohydrates on the surface of nonuniform (complex) substrates is of the prime interest for many applications.

The results for the adsorption isotherm for FITC-ZZ-CBM1$_{Hj\text{Cel7A}}$ on Avicel showed a reasonable fit to the standard Langmuir curve (Figure 4.) suggesting a standard specific and reversible binding mode. A K_d value of 4.1 ± 1 μM and B_{max} value of 540 ± 108 pmol/mg was also in reasonable accordance with data reported for similar measurements.[25]

Using typical non-saturating conditions, i.e., with an initial protein concentration more than 1 order of magnitude below K_d, it is possible to calculate the amount B_{max} of binding sites from the linear part of an adsorption isotherm:

$$B_{\text{Max}} = \text{Bound}\frac{K_d}{\text{Free}}$$

where B is amount of bound $CBM1_{HjCel7A}$ (mol/g) and Free is the concentration of unbound CBM in the supernatant (M).

It has been shown previously that oxygen delignification of kraft pulp causes a gradual decrease in cellulose crystallinity.[51,57] Incubation of $CBM1_{HjCel7A}$ with different pulp samples demonstrated that the amount of CBM adsorbed clearly depended on the type of pulp. Significantly lower adsorption was recorded for the bleached pulp compare to unbleached pulp suggesting a modification of the sites for binding after the bleaching process (Table 2).

Thus the fluorescent assay developed represents an appropriate method for quantitative analysis of available binding sites for ZZ-$CBM1_{HjCel7A}$ on nonuniform pulp fiber surfaces.

Conclusions

The data obtained shows that CBMs can be used for specific and efficient labeling of different cell wall components on plant tissues samples and pulp fiber surfaces. Owing to their high specificity and small size, CBMs are able to access the different cell wall carbohydrates with higher precision than antibodies that are much larger molecules. Moreover, the data obtained with two different mannan specific CBMs suggest that even small differences in the specific structure of the substrates can be detected in complex plant tissues and fibers. CBMs thus provide a novel means that may be used for the sensitive detection of changes in the distribution of carbohydrates on pulp surfaces after different types of chemical and mechanical processing or for determining the distribution, composition, and structures of cell wall carbohydrates in, e.g., genetically modified plant cell walls.

Acknowledgment. The pET28a *Escherichia coli* expression vector containing the TmCBM27 insert was a kind gift from Dr. Alisdair B. Boraston, Victoria, Canada, and the pET22b *E. coli* expression vector containing the CjCBM35 was a kind gift from Dr. Harry Gilbert, Newcastle, U.K. This work was carried out within the framework of the Wood Ultrastructure Research Centre (WURC), a VINNOVA (NUTEK) competence centre at the Swedish University of Agricultural Sciences (http://www-wurc.slu.se/).

References and Notes

(1) Boudet, A. M.; Kajita, S.; Grima-Pettenati, J.; Goffner, D. *Trends Plant Sci.* **2003**, *12*, 576-581.
(2) Tang, W.; Luo, X.; Nelson, A.; Collver, H.; Kinken, K. *Genomics Proteomics Bioinf.* **2003**, *1*, 263−278.
(3) Ralph, J.; Guillaumie, S.; Grabber, J. H.; Lapierre, C.; Barriere, Y. *C. R. Biol.* **2004**, *327*, 467−479.
(4) Somerville, C.; Bauer, S.; Brininstool, G.; Facette, M.; Hamann, T.; Milne, J.; Osborne, E.; Paredez, A.; Persson, S.; Sjöberg, J.; Kleen, M.; Dahlman, O.; Adnemo, R.; Sundvall, H. *Nord. Pulp Pap. Res. J.* **2004**, *19*, 392−396.
(5) Shevell, D. E.; Kunkel, T.; Chua, N. H. *Plant Cell* **2000**, *12*, 2047−2060.
(6) Sjöberg, J.; Kleen, M.; Dhalman, O.; Agnemo, R.; Sundsvall, H. *Nord. Pulp Pap. Res. J.* **2004**, *19*, 392−396.
(7) Neto, C. P.; Silvestre, A. J. D.; Evtuguin, D. V.; Freire, C. S. R.; Pinto, P. C. R.; Santiago, A. S.; Fardim, P.; Holmbom, B. *Nord. Pulp Pap. Res. J.* **2004**, *19*, 513−520.
(8) Daniel, G. *ACS Symp. Ser.* **2003**, *845*, 34−72.
(9) Daniel, G.; Volc, J.; Niku-Paavola, M. L. *C. R. Biol.* **2004**, *327*, 861−871.
(10) Duchesne, I.; Takabe, K.; Daniel, G. *Holzforschung* **2003**, *57*, 62−68.
(11) Knox, J. P. *Int. Rev. Cytol.* **1997**, *171*, 79−120.
(12) Goldblett, D. *J. Med. Microbiol.* **1988**, *47*, 563−567.
(13) Rudiger, H., Gabius, H. L. *Glycoconjugate J.* **2001**, *18*, 589−613.
(14) Ambrosi, M.; Cameron, N. R.; Davis, B. G. *Org. Biomol. Chem.* **2005**, *3*, 1593−1608.
(15) Boraston, A. B.; Bolam, D. N.; Gilbert, H. J.; Davies, G. J. *Biochem. J.* **2004**, *382*, 769−781.
(16) Bolam, D. N.; Ciruela, A.; McQueen-Mason, S.; Simpson, P.; Williamson, M. P.; Rixon, J. E.; Boraston, A.; Hazlewood, G. P.; Gilbert, H. J. *Biochem. J.* **1998**, *331*, 775−781.
(17) Carrard, G.; Koivula, A.; Söderlund, H.; Béguin, P. *Proc. Natl. Acad. Sci. U.S.A.* **2000**, *97*, 10342−10347.
(18) Boraston, A. B.; Ghaffari, M.; Warren, A. J.; Kilburn, D. G. *Biochem. J.* **2002**, *361*, 35−40.
(19) McCartney, L.; Gilbert, H. J.; Bolam, D. N.; Boraston, A. B.; Knox, J. P. *Anal. Biochem.* **2004**, *326*, 49−54.
(20) Kraulis, J.; Clore, G. M.; Nilges, M.; Jones, T. A.; Pettersson, G.; Knowles, J.; Gronenborn, A. M. *Biochemistry* **1989**, *28*, 7241−7257.
(21) Hashimoto, M.; Ikegami, T.; Seino, S.; Ohuchi, N.; Fukada, H.; Sugiyama, J.; Shirakawa, M.; Watanabe, T. *J. Bacteriol.* **2000**, *182*, 3045−3054.
(22) Tormo, J.; Lamed, R.; Chirino, A. J.; Morag, E.; Bayer, E. A.; Shoham, Y.; Steitz, T. A. *EMBO J.* **1996**, *15*, 5739−5751.
(23) Linder, M.; Teeri, T. T. J. *Biotechnology* **1997**, *57*, 15−28.
(24) Boraston, A. B., McLean, B. W., Guarna, M. M., Amandaron-Akow, E., Kilburn, D. G. *Protein Expression Purif.* **2001**, *21*, 417−423.
(25) Hilden, L.; Daniel, G.; Johansson, G. *Biotechnol. Lett.* **2003**, *25*, 553−558.
(26) McCartney, L.; Blake, A. W.; Flint, J.; Bolam, D. N.; Boraston, A. B.; Gilbert, H. J.; Knox, J. P. *Proc. Natl. Acad. Sci. U.S.A.* **2006**, *103*, 4765−4770.
(27) Druzhinina, I.; Kubicek, C. P. *J. Zhejiang Univ. Sci. B.* **2005**, *6*, 100−112.
(28) Lehtiö, J.; Sugiyama, J.; Gustavsson, M.; Fransson, L.; Linder, M.; Teeri, T. T. *Proc. Natl. Acad. Sci. U.S.A.* **2003**, *100*, 484−489.
(29) Boraston, A. B.; Revett, T. J.; Boraston, C. M.; Nurizzo, D.; Davies, G. J. *Structure* **2003**, *11*, 665−675.
(30) Bolam, D. N.; Xie, H.; Pell, G.; Hogg, D.; Galbraith, G.; Henrissat, B.; Gilbert, H. J. *J. Biol. Chem.* **2004**, *279*, 22953−22963.
(31) Hogg, D.; Pell, G.; Dupree, P.; Goubet, F.; Martin-Orue, S. M.; Armand, S.; Gilbert, H. J. *Biochem. J.* **2003**, *371*, 1027−1043.
(32) Srisoduk, M.; Lehtiö, J.; Linder, M.; Margolles-Clark, E.; Reinikainen, T.; Teeri, T. T. J. *Biotechnology* **1997**, *57*, 49−57.
(33) Tomme, P.; Boraston, A.; Kormos, J. M.; Warren, R. A. J.; Kilburn, D. G. *Enzyme Microb. Technol.* **2000**, *27*, 453−458.
(34) Gilkes, N. R.; Jervis, E.; Henrissat, B.; Tekant, B.; Miller, R. C., Jr.; Warren, R. A.; Kilburn, D. G. *J. Biol. Chem.* **1992**, *267*, 6743−6749.
(35) Timell, T. E. *Sven Papperstidn.* **1969**, *6*, 173−181.
(36) Kaakinen, S.; Kostiainen, K.; Ek, F.; Saranpää, P.; Kubiske, M. E.; Sober, J.; Karnosky, D. F.; Vapaavuori, E. *Global Change Biol.* **2004**, *10*, 1513−1525.
(37) Meier, H. *J. Polym. Sci.* **1961**, *51*, 11−18.
(38) Solo, M. L. *Aikakawsh* **1965**, *37*, 127.
(39) Allsopp, A.; Misra, P. *Biochem. J.* **1940**, *34*, 1078−1084.
(40) Theliander, H.; Brelid, H.; Wigell, A. Kinetics of the Dissolution of Hemicellulose from Softwood under Alkaline Conditions. The 2005 Annual Meeting (Cincinnati, OH), Forest Products Division (17), session #545.
(41) Schramm, M.; Hestrin, S. J. *Gen. Microbiol.* **1954**, *11*, 123−129.
(42) Ander, P.; Nyholm, K. In *Proceedings of the International Symposium on Wood Machining Properties of Wood and Wood Composites related to Wood Machining*, 27−29. September 2000, Vienna, Austria. Eds: Stanzl-Tschegg and A. Reiterer, pp 3−19.
(43) Bardage, S., Donaldson, L., Tokoh, C., Daniel, G. *Nord. Pulp Pap. Res. J.* **2004**, *19*, 449−452.
(44) Linder, M.; Teeri, T. *Proc. Natl. Acad. Sci. U.S.A.* **1996**, *93*, 12251−12255.
(45) Carrard, G.; Linde, M. *Eur. J. Biochem.* **1999**, *262*, 637−643.
(46) Ståhlberg, J.; Henriksson, H.; Divne, C.; Isaksson, R.; Pettersson, G.; Johansson, G.; Jones, T. A. *J. Mol. Biol.* **2001**, *305*, 79−93.
(47) Tomme, P.; Driver, D. P.; Amandoron, E. A.; Miller, R. C.; Warren, R. A. J.; Kilburn, D. G. *J. Bacteriol.* **1995**, *177*, 4356−4363.
(48) Pilate, G.; Chabbert, B.; Cathala, B.; Yoshinaga, A.; Leple, J. C.; Laurans, F.; Lapierre, C.; Ruel, K. *C. R. Biol.* **2004**, *327*, 889−901.

(49) Prodhan, A. K. M. A.; Funada, R.; Ohtani, J.; Abe, H.; Fukazawa, K. *Planta* **1995**, *196*, 577−585.
(50) Côte, W. A., Jr.; Day, A. C. *Syracuse, NY: Syracuse University Press* **1965**, 391−418.
(51) De, Souza, J.; Bouchard, J.; Méthot, M.; Berry, R.; Argyropoulos, D. S. *J. Pulp Pap. Sci.* **2002**, *28*, 167−170.
(52) Sunna, A.; Gibbs, M. D.; Bergquist, P. L. *Biochem. J.* **2001**, *356*, 791−798.
(53) Roske, Y.; Sunna, A.; Pfeil, W.; Heinemann, U. *J. Mol. Biol.* **2004**, *340*, 543−554.
(54) Stoll, D.; Boraston, A.; Stålbrand, H.; McLean, B. W.; Kilburn, D. G.; Warren, R. A. J. *FEMS Microbiol. Lett.* **2000**, *183*, 265−269.
(55) Freelove, A. C. J.; Bolam, D. N.; White, P.; Hazlewood, G. P.; Gilbert, H. J. *J. Biol. Chem.* **2001**, *276*, 43010−43017.
(56) Tunnicliffe, R. B.; Bolam, D. N.; Pell, G.; Gilbert, H. J.; Williamsson, M. P. *J. Mol. Biol.* **2005**, *347*, 287−296.
(57) Liitia, T. M.; Maunu, S. L.; Hortling, B.; Toikka, M.; Kilpelainen, I. J. *Agric. Food Chem.* **2003**, *51*, 2136−2143.

BM060632Z